The unprecedented ozone loss in the Arctic winter and spring of 2010/2011 and 2019/2020

Divakaran Ardra[1,2], Jayanarayanan Kuttippurath[1,*], Raina Roy[1,2], Pankaj Kumar[1], Sarath Raj[1], Rolf Müller[3] and Wuhu Feng[4, 5]

[1]*CORAL, Indian Institute of Technology Kharagpur, Kharagpur, 721302, India*

[2]*Department of Physical Oceanography, Cochin University of Science and Technology, Kochi.*

[3]*Forschungszentrum Jülich GmbH (IEK-7), 52425 Jülich, Germany*

[4]*National Centre for Atmospheric Science, University of Leeds, Leeds, LS2 9PH, UK*

[5]*School of Earth and Environment, University of Leeds, Leeds, LS2 9JT, UK*

*Corresponding author: jayan@coral.iitkgp.ac.in

HIGHLIGHTS

- A close comparison between the exceptional Arctic winters 2020 and 2011
- Long-lasting vortex up to the end of April in 2020, but up to early April 2011
- Unusually early chlorine activation and ozone loss in early January 2020
- The ozone loss in 2020 is stronger in lower stratosphere than that in 2011

Key words: Climate Change; Arctic ozone; Polar Vortex; Ozone hole; Satellite measurements; Ozonesonde

Short title: Ozone loss in the Arctic winters 2011 and 2020

ABSTRACT

Polar ozone depletion has been a major environmental threat for humanity since the late 1980s. The 2011 Arctic winter caught much global attention because of the amount of ozone loss (2.3–3.4 ppmv at 450–475 K potential temperature) and a similar loss was also observed in the 2020 winter (2.5–3.5 ppmv, at 400–500 K). Since the difference between the winter of 2010/11 and 2019/20 in terms of ozone loss is small, we investigate the change in terms of polar processing in these winters, as that would help future projections of ozone recovery in polar regions. The ozone loss estimated by different methods (passive tracer and vortex descent) shows the highest loss in April in both years 2011 and 2020, but the peak ozone loss altitude was different. The overall ozone loss was more extensive in the lower stratosphere in 2020, but relatively large loss occurred at higher altitudes in 2011. A prolonged chlorine activation was evident in 2020, longer than that in 2011, which also enhanced loss in the lower stratosphere in 2020. The situation in 2020 resulted in very small values of column ozone, which were below 220 DU for more than three weeks, and a near-complete ozone loss (93%) at certain altitudes in the lower stratosphere. The ozone loss in 2020 was similar to that in the Antarctic, and was triggered by the presence of a strong and stable polar vortex with zonal winds of constant velocity (40–45 ms^{-1}) and temperature conditions favoring large areas of PSCs (10 million km^2) for most of the winter. The relatively lower values of momentum flux suggest that the tropospheric forcing was lower in 2020. Therefore, both winters had less disturbed and long-lasting polar vortices allowing lower temperatures, large areas of PSCs, and longer periods of severe chlorine activation, which in turn led to record-breaking ozone loss of the levels found in the Antarctic vortex, for some days.

1. INTRODUCTION

Polar stratospheric ozone loss has been a severe threat since the Antarctic ozone hole was discovered in 1985[1]. The formation of the ozone hole resulted from emissions of ozone-depleting substances (ODSs) like CFCs, bromo-halides and several other compounds originating from human activities[2–6]. The lower temperatures and isolated air masses inside vortex in the Antarctic made the ozone hole an annually recurring event, unlike in the Arctic[7,8]. The interannual variability of the relative strength of Arctic vortex[9] and the presence of higher temperature due to greater transport and mixing from the lower latitudes[10,11] significantly affect the extent of Arctic ozone depletion. For strong polar chemical ozone depletion to occur, it is necessary that not only sufficiently low temperatures are reached at some point in winter/spring, but also that such low temperatures, as well as high active chlorine levels, are sustained into spring. The polar regions experience the strongest ozone loss in spring (late August, September, early October in the Antarctic; late February, March, early April in the Arctic)[12]. During these periods, high active chlorine levels need to be sustained at a time when both gas-phase chlorine deactivation and heterogeneous chlorine activation proceed at large rates[13–16]. Arctic ozone loss has been prevalent since the late eighties[17,18]. The ozone loss, however, is less pronounced than in the Antarctic because of the meteorology of the Arctic winters, which is different from that of Antarctic winters[10,19].

The stratosphere in the Arctic during winter is subject to frequent tropospheric wave forcings in the Northern Hemisphere (NH), and thus, culminates in Sudden Stratospheric Warming (SSW) in many winters[20]. This warming reduces ozone depletion by weakening the polar vortex[21–23]. Strong Arctic ozone loss is common in cold winter/spring[24–26]. Studies showed that the mean PSC volume (V_{psc}) and the area of PSC (A_{psc}) in the Arctic in cold winters have been increasing since the late 1960s. This increase in PSC volume directly implies an accelerated loss of ozone as it facilitates the activation of chlorine in the presence of sunlight[27]. This increasing depletion of ozone in the Arctic is hypothesized to climate change in the stratosphere, and every one degree of cooling will result in an additional ozone loss of 15 DU[26,28]. A

similar conclusion was derived in several other studies from the Arctic ozone loss observations[29]. The combination of greenhouse gas (GHG) forcing and the subsequent cooling of the stratosphere has a direct impact on the stability of the Arctic polar vortex, and is found to remarkably increase the ozone loss[30–33]. The most recent study of von der Gathen et al.[34] concludes that if the future abundance of GHGs continues to rise, it would favor a large seasonal loss of Arctic ozone. Sinnhuber et al.[35] report that cooling of 0.8 K/decade in the Arctic winter stratosphere would counterbalance the effects of reduced stratospheric halogen loading due to the Montreal Protocol. A similar offset in the predicted ozone recovery due to projected stratospheric radiative cooling is also presented in the study of Bohlinger et al.[36] The shift of polar minimum temperatures from late to early winters would induce early formation of the polar vortex. Therefore, it would contribute to enhanced and prolonged ozone loss in the Arctic, as mentioned in the study of Langematz et al.[37]. The central Pacific Sea Surface Temperature (SST) warming also influences the depletion of ozone in the Arctic, which contributes to the strengthening of Arctic vortex in winter (DJF)[38]. Also, the negative SST phase leads to strengthening of the vortex as found in 2011 due to a reduction in the planetary wave propagation[39–41].

A strong chemical ozone loss caused by a long period of low temperature in the lower stratosphere is rare in the Arctic, and the earliest such ozone loss was reported for the 1995/96 winter, followed by 1996/97, 1999/2000, 2010/11, 2015/16, and 2019/20[28,42–44]. Chemical ozone loss in the Arctic in 1997 was supported by PSC formation and a strong polar vortex that persisted until late April[45–47]. Similar winter conditions occurred more extremely in the 2011 winter. The ozone loss was very severe such that the situation that usually experiences in the Antarctic was observed[8,11,29,35,44,48,49]. The ozone loss estimated was in the order of 2.3–3.5 ppmv in late March-early April 2011, though the value differed slightly in these studies due to differences in defining the vortex edge criterion, measured altitude ranges, and the methods used to calculate the ozone loss. The 2015/16 winter was also distinct, but the vortex was not long lasting, as it dissipated in early March 2016 due to the early final warming[50]. The temperature

observed from December 2015 through early February 2016 was the lowest in the past 68 years, which caused severe denitrification and high dehydration[50–52]. The 2020 winter also exhibited characteristics similar to the previous extreme cold winters of the Arctic (i.e., 1996/97 and 2010/11). The winter showed the lowest temperature record for the past 41 years, a strong vortex that lasted until late April[53], ozone loss rising to values similar to those observed in the 2011 winter[54–58], and strong denitrification. Model studies of the 2020 winter also arrived at similar conclusions[59–61]. Here, we present an in-depth analysis of polar processing in both 2011 and 2020 winters and discuss the similarities and differences, as this would help modeling studies and future projection of ozone recovery in the Arctic.

2. DATA AND METHODS

We use the satellite measurements of ozone, N_2O and ClO from Microwave Limb Sounder (MLS) v5[62,63]. The MLS profiles are presented in potential temperature vertical co-ordinates. It is computed using the pressure and temperature data available from the MLS profiles. The MLS temperature, ozone, N_2O and ClO data have an uncertainty of 2–10%, depending on the constituent, latitude and altitude region. The potential vorticity (PV) values are taken from the European Centre for Medium-Range Weather Forecasts (ECMWF) Reanalyses ERA5 data[64]. The ozone loss calculation is performed inside the vortex, and the vortex edge at different altitudes is determined using to the Nash et al.[65] criterion.

The vertical distribution of N_2O is exponential due to the photolysis and lack of N_2O sources in the lower altitudes. The MLS N_2O data extracted from 190 GHz retrieval provides information at a pressure level of 68 hPa (or 400 K isentropic level). Subsequently, the data are extrapolated to 350 K by an exponential fitting to the N_2O data for the 400–600 K levels. Profile descent method[66–69] is applied for the estimation of ozone loss, in which the N_2O data are used for descent calculations. The ozone loss is estimated by utilizing the ozone profiles in December of the preceding year. Apart from this, ozone loss is also calculated with the passive method for which a passive tracer from the SLIMCAT simulations is used[67,70,71]. The depletion is computed for each day for which the ozone measurements are subtracted from the

tracer each day. The meteorology of the winter is analyzed using the Modern-Era Retrospective analysis for Research and Applications version 2 (MERRA-2) data[72], and these data are available for the period 1980–2021.

3. RESULTS AND DISCUSSION

3.1 Meteorology of the winters 2020 and 2011. Figure 1 shows the monthly evolution of different meteorological parameters for the years 2011 (black) and 2020 (green) along with the average for the period 1980–2020 (red) in the Arctic. The top panel shows the evolution of zonal mean minimum temperature for 50–90°N at 50 hPa and it is interesting to observe temperatures less than 195 K (indicated by the black line) (see Grooß and Müller[61]; figure 10) for nearly four months in both years, which is rare in the Arctic. The regions of lower temperature are significant as they are important for the formation of PSCs. These clouds further help in the process of ozone loss by serving as the activation surface for chlorine[73]. The winters had a minimum temperature less than the PSC existence threshold from December to March and started to rise above this value by early April, consistent with the results of previous studies (e.g., Figure 1 of Manney et al.[44,55]). Kuttippurath et al.[48] and Varotsos et al.[74] used the zonal average of minimum temperatures from 40° to 90° N at 475 K and observed a similar evolution of minimum temperatures below the PSC threshold for 2011. Dameris et al.[75] analyzed the mean monthly minimum temperature at 50 hPa for the zonal average between 50° N and 90° N, and it showed that the temperature was less than 195 K during December–March in both years. The values of temperatures during the winter months are lower in 2020 (see also Alwarda et al.[76]). On the other hand, the long-term mean (1980–2020, red curve) shows PSC favorable temperatures only in December and January. The second panel shows the development of zonal mean temperature at 60°–90° N. In 2020, the temperature decreased from 210 K in early December to 204 K by mid-January. This drop, however, has been compensated by a rise of the same amount towards late January 2020. The temperature shows a consistent value for at least a month thereafter, but increases by mid-March. Temperature values are

158 lowest in late February 2020 and are observed to be the lowest since 1979[53]. The winter 2020 shows
159 lower temperature values in the order of 205–208 K in the third week of February. In 2011, there were
160 two small peaks in temperature in early January and early February (see Kuttippurath et al.[48]). As
161 compared to these, only one minor warming was observed in 2020, from late January to early February.

162 The third panel of Figure 1 compares the PSC area for both winters and the mean PSC area from 1980 to
163 2020 (red). The PSC area at 460 K spreads to 14 million km^2 in late January 2020 and stands slightly higher
164 than that in 2011 throughout the period until mid-March. The PSC area stayed around 8–10 million km^2
165 for most of December, January, February, and March in both years, and was similar to that observed in
166 the Antarctic[58,77]. The mean PSC area stayed less than 5 million km^2 throughout the years. An associated
167 drop in the PSC area in both winters was observed concurrent with the periods of minor warming.

168 The bottom fourth panel shows the relative strength of polar vortex in terms of zonal wind velocity (U).
169 Lawrence et al.[53] described the 2020 winter vortex to be the largest with an area of 20–25 million km^2
170 and that lasted until late April. The zonal winds in both winters follow a constant velocity of about 30–40
171 ms^{-1} up to late March, which is not usually observed in the Arctic winters (see Lawrence et al.[53]). The
172 uniformity in wind speed ensures a strong polar vortex and the final warming with reversal of westerlies
173 happened around mid-April in 2011 and late April in 2020[78]. The zonal wind speed at 100 and 10 hPa in
174 2020 are the highest and third highest, respectively, when compared to the winters since 1959[53]. Thus,
175 the vortex during both winters was long lasting and stronger in 2020. A comparison of the maximum PV
176 at 475 K from 1994 to 2012 showed that the PV gradient was sharpest in 2011; indicating that the vortex
177 strength was highest in that winter[29].

178 The last two panels of figure 1 examine the momentum and heat fluxes during the years (2011 and 2020)
179 along with the climatology values (red). The momentum flux estimates at 60° N (100 hPa) for both years
180 show that flux is mostly negative during December, January and February (DJF), suggestive of a relatively

stable polar vortex. However, it is observed that the climatology values are only slightly negative (-15 m^2s^{-2}). Beyond DJF, the values become positive; indicating increased wave forcing and a less stable polar vortex. The bottom panel of Figure 1 illustrates the zonally averaged 45-day mean heat flux computed over the latitude region 45–75° N at 100 hPa. Heat fluxes in both winters are found to be below the mean or climatology values until mid-April. Although the flux is directed poleward during most of the winter, the range of values is small, and henceforth, the vortex was more stable in 2011 and 2020; consistent with the analyses of Inness et al.[54]. The model simulations performed by Rao and Garfinkel[79] also predict a very stable polar vortex in the 2020 winter similar to that observed in 2011 and 1997. Lee et al.[80] reveals that a possible reason for the relatively low wave forcing during the winter is due to the destructive interference of tropospheric waves with the climatological stationary waves in the early winter of 2020.

3.2 Evolution of the Polar Vortex. Figure 2 shows the temporal evolution of the polar vortex in both winters. The days are chosen such that the vortex begins to form in early December and becomes fully formed by late January. In the following months, the vortex splits or displaces in the presence of strong SSW, and remains relatively stable in the absence of SSWs. The top panel of the figure shows the initial formation of the vortex in 2011. A complete and distinct vortex forms towards the end of January despite the minor warming. The warming intensified in February when the vortex split into two parts. The vortex recovered soon after the temperature lowered and thus, reformed a pole-centered circular vortex thereafter in early March. It remained intact until early April, which was in agreement with the previous studies[48]. In 2020, a large vortex was formed in early January as illustrated in the PV maps. The areal spread of vortex was larger in 2020 than that in the 2011 winter. The prolonged appearance of low temperatures, which is quite unusual compared to the observations in the past 41 years (1979/80 - 2019/20), led to a strong and stable vortex in 2020[56]. Despite the minor warming in late January, the vortex remained strong until late April. Eventually, at the end of April, the vortex splits into two lobes. The location of vortex in either of these winters was pole-centered although its spatial spread extended up to

the mid-latitudes[75]. A detailed comparison of relevant meteorological parameters for both winters is presented in Table 1.

Important parameters that possibly affect the strength of polar vortex are the external influences, such as Quasi-Biennial Oscillation (QBO), El Nino Southern Oscillations (ENSO), Eurasian snow cover, solar cycle, and several others[81–83]. The strength of the vortex is higher in the westerly phase of QBO (in the tropical lower stratosphere at ~50 hPa) by the Holton-Tan relationship[84]. The QBO was westerly during the 2011 winter[85]. The QBO and ENSO were both nearly neutral in the 2020 winter[79]. The 2011 winter witnessed the La Nina phase[86]. Thus, these external influences also impacted positively on the vortex by reducing the severity of tropospheric forcing and thus, strengthening the vortex.

3.3 Diabatic Descent and Chlorine Activation in 2020 and 2011. Figure 3 shows the distribution of O_3, ClO, N_2O, and HNO_3, derived for the winters using satellite observations. Data corresponding to the temporal evolution of trace gases are obtained from MLS on the Aura satellite. There is a substantial increase in the concentration of N_2O in the lower stratosphere, indicating the dynamic descent in the stratosphere. The descent rate is greater in 2020 than in 2011 when the N_2O isolines are followed (third panel of Figure 3, also see Feng et al.[60]). The N_2O values decrease rapidly to as low as 50 ppbv from 250–300 ppbv at 400 K altitude from December to April in 2020, but the range of values stays around 150–250 ppbv at 400 K in 2011. Similar diabatic descent rates in 2020 are also reported by Grooß and Müller[61] using CLaMS simulations and ACE-FTS measurements. However, that study was carried out for the days between 23 and 29 March, and the simulations showed slower descent, though the range is similar to that in our analysis. Manney et al.[55] observed a lower than normal concentration of N_2O in the lower stratosphere in 2020, which was caused by the increased descent from the mid-stratosphere.

In general, chlorine activation in the Arctic begins in early January and continues until late February[43]. The period of activation implies a strong association between PSC existence and the temperatures of chlorine

228 activation. The highest chlorine activation is observed during the coldest periods of the winters; i.e.,
229 January and February. In 2011, the ClO concentrations reached 1.6 ppbv in January and the chlorine
230 activation was present up to late March when the ClO values dropped to less than 1 ppbv (500–600 K).
231 Conversely, the ClO concentration was higher than 1.7 ppbv in late December 2020 at 500–600K[55]. Unlike
232 the usual winters, the enhanced concentration of ClO in 2020 was not only restricted to the altitudes at
233 500–550 K, but also was present between 500 and 600 K for almost a month. The chlorine levels declined
234 soon after January 2020 and were negligible in early February 2020. A possible reason that decelerated
235 the chlorine activation is the minor warming in early February 2020. However, the chlorine activation in
236 2011 continued even after January and persisted until late March (500–550 K). Therefore, similar to the
237 results of Manney et al.[55] chlorine activation in the higher altitudes was stronger in 2011 than in 2020
238 (see also Inness et al.[54]). The ozone loss during the winters is comparable because of the compensating
239 spatial distribution of ClO in both winters. The record-high chlorine activation observed in 2011 is also
240 discussed in Adams et al.[87] and Kuttippurath et al.[48].

241 The 2020 winter shows a proportional relationship between the period of lowest temperature and severe
242 denitrification. The concentration of HNO_3 is important to analyze the denitrification in the period. The
243 concentration of HNO_3 in the lower stratosphere was above 12 ppbv in early December 2011, compared
244 to 9 ppbv in 2020. The seasonal evolution from winter to spring further reduces the concentration of
245 HNO_3 due to photolysis[88]. The concentration of HNO_3 in early spring is lower by about 60–80% than in
246 early winter 2020[57], opposed to the 40–50% denitrification in 2011[35,48]. The minor warming in late
247 January subsides the rate of denitrification for that particular period in 2020. The bottom panel of figure 3
248 shows the temporal evolution of ozone concentration. The maximum concentration of ozone is limited to
249 the middle (550–700 K) and upper stratosphere (850 K and above) whereas the lowest ozone
250 concentration occupies the 350–500 K altitude region (lower stratosphere). The denitrification was severe
251 in both winters of 2011 and 2020. A similar rate of high vortex-wide denitrification had also been

252 reported in the Arctic winter 2016[29,44,89]. The highest ozone concentration in Figure 4 is observed in the
253 upper stratosphere in both years and is the highest in April for 2020 (5–6 ppmv) and March for 2011 (4–5
254 ppmv) (note that the MLS data are not available in April 2011). The smallest concentration of ozone is
255 observed in the lower stratosphere and is lower than 1 ppmv. The period of lowest concentration is found
256 to be coherent with the period of peak chlorine activation and denitrification.

257 The increased rate of vortex descent, accelerated denitrification and enhanced chlorine activation in
258 2020, make it more conducive for the large ozone loss. The ozone concentrations began to decline earlier
259 in 2020 and the loss was also slightly higher than that in 2011 in the lower stratosphere, below 550 K. The
260 loss was observed at 400–650 K in December and the loss became more apparent in the lower
261 stratosphere thereafter in the minor warming period. The amount of ozone in the lower stratosphere is
262 between 1 and 3 ppmv in both winters in December, but it reduced to less than 1.5 ppmv in March and
263 April, as depicted in the figures. The difference between both winters is mostly about the onset of loss
264 and the peak ozone loss period. The unusual ozone loss since December is very particular to 2020 and the
265 loss is slightly higher in 2020 than that in 2011. The measurements show exceptionally smaller values of
266 ozone, about 0.5 ppmv or below, from mid-March to the end of April at 350–450 K in 2020. Due to the
267 unavailability of MLS data in April 2011, a gap is shown in the analyses for that period, which also makes
268 the comparison between the winters for the period slightly difficult. The lowermost panel of Figure 4
269 shows the difference in the concentration of ozone in both winters and is mostly smaller than 1 ppmv.

270 **3.4 Ozone loss in the winters 2020 and 2011.** A method suitable to calculate the chemical ozone loss
271 neglecting the impact of the mixing process and other dynamic processes is the vortex descent
272 method[69,90]. We have analysed the chemical ozone loss by applying the vortex descent method. In
273 addition, the passive tracer method is also used to calculate ozone loss. The ozone loss is computed by
274 finding the difference of passive ozone simulated from SLIMCAT from measured ozone[91]. Figure 4 shows

the chemical ozone loss estimated using the MLS measurements for the winters 2020 and 2011. The ozone loss as mentioned previously is estimated by the vortex descent and by the passive method using the simulations from the chemical transport model (CTM), SLIMCAT[92]. As the ozone loss is evaluated with respect to the MLS data, there is a corresponding gap in 2011 due to the lack of measurements in early April 2011.

The ozone loss reached a maximum of 2.4 ppmv at 350–475K in March 2011. The loss in the lower stratosphere shows more than 2.5 ppmv in March 2020. In the middle stratosphere above 450 K, the ozone loss is larger in 2011 than that in 2020. However, the ozone loss in the upper stratosphere shows a similar value in both winters. The difference in the ozone loss between the winters is that it stays around +(0.2–0.5) ppmv in 2020 compared to less than -(0.6–0.7) ppmv in 2011 in the middle stratosphere. The ozone loss estimated by the passive method for the winter 2011 by Manney et al.[44], Kuttippurath et al.[48], Sinnhuber et al.[35], and Griffin et al.[69] shows about 2.1–2.5 ppmv at 450–550 K. The ozone loss estimated by Wohltmann et al.[56] shows 2.2 ppmv at 450K in 2020 and 2.5 ppm at 490 K in 2011. They find that the ozone loss amount in the 2011 winter was higher probably because of the greater transport of ozone from lower altitudes in that winter, though the percentage of ozone loss was higher in 2020 (73%) than that in 2011 (63%). The 2011 ozone loss determined by the Match method in the study of Livesey et al.[93] presented a loss of 2.0 ppmv at 450 K. Manney et al.[55] estimated the ozone loss for both winters using the Match method and found a loss of about 2.8 ppmv in the lower stratosphere. They also showed that the loss in lower altitudes in 2020 was larger than that in 2011; consistent with the results from the studies by Kuttippurath et al.[57], Inness et al.[54], Grooß and Müller[61], and Dameris et al.[75], although there is a slight difference in the loss calculated in percent. Figure 6 summarizes and further compares the ozone losses in various studies for both winters.

297 The vertical profiles show an early onset of the ozone loss in the upper stratosphere in December of the
298 order of 0.5–0.6 ppbv in 2020, but close to zero in 2011 (Figure 5). In the lower stratosphere, the ozone
299 loss situation in both years is similar in December with little loss. The ozone loss occurred in January and
300 February is higher in 2020, and the loss reached up to 1.5 ppbv in January and 2.5 ppbv in February 2020.
301 In 2011, the loss was less than 0.5 ppbv, and the pattern of loss is the same in the upper stratosphere in
302 both years, even though the standard deviation is higher in 2020. The highest ozone loss was measured in
303 the lower stratosphere in April followed by March in 2020[54,57]. The loss in April 2020 was about 2.5 ppbv
304 though the standard deviation reaches up to 3.5 ppbv. However, the loss is very small and is close to zero
305 in the upper stratosphere. The interesting aspect here is that there is higher ozone loss compared to the
306 previous winters in the upper stratosphere, about 0.5 ppbv in March and April in both winters; which
307 suggests the relatively higher ozone loss in these years.

308 To examine the extreme ozone loss in these winters, we considered the total column ozone (TCO, Figure
309 6). The ozone maps clearly show that the values never dropped below 220 DU on any day in 2011, but
310 there were more than three weeks in which TCO dropped below that threshold in 2020. The severity of
311 this winter and extreme ozone loss is further investigated using ozonesonde measurements (bottom,
312 Figure 6). The ozonesonde measurements at Alert and Eureka show near-complete loss of ozone or loss
313 saturation in 2020 in some days (80–93% loss). Conversely, the ozonesonde measurements in 2011 never
314 experienced the loss saturation or such low ozone values as observed in 2020 at any altitude. Therefore,
315 both total column and ozonesonde measurements attest that the winter 2020 was unprecedented and
316 was colder, denitrified, chlorine activated and ozone depleted than those in 2011.

317 ## 4. CONCLUSION

318 The very strong Arctic ozone loss in the 2020 winter has turned out to be a matter of severe interest for
319 the human community globally[94]. Bernhard et al.[95] observed a 140% increase in the measurements of the

ultraviolet index (UVI) for several days in 2020 compared to previous years. The severe ozone loss in the Arctic would affect a major part of the population in the surrounding land regions[34,96]. There are studies that show that stratospheric ozone is recovering globally, but not in the Arctic, yet[12,62]. The reason is the reduction of atmospheric chlorine levels caused by the Montreal Protocol and its amendments and adjustments. Arctic ozone would have developed into an Antarctic-like ozone hole if not for the Montreal Protocol[97]. The 2020 winter showed severe ozone loss in the order of 2.5 ppmv in the altitude range between 400 and 500 K. The magnitude of the loss in 2011 was slightly lower and remained to same altitude range, particularly below 475 K. The conditions that made 2020 winter conducive to ozone loss were the long-lasting low temperatures in the lower stratosphere, where the minimum temperature remained below the PSC existence threshold for more than a month, giving rise to large areas of PSCs and a prolonged severe chlorine activation. The early start of the ozone loss in 2020 as compared to that in 2011 is identified by the beginning of PSC formation. The vortex in both winters remained undisturbed until early April and late April in 2011 and 2020, respectively. Thus, our study indicates that winter 2020 had a very low temperature, long-lasting and undisturbed vortex, slightly higher chlorine activation and larger ozone loss than that in 2011. In 2020, the Arctic winter also experienced a near-complete loss of ozone and TCO values lower than 220 DU for more than 23 days. The comparison of the Arctic winters of 2011 and 2020, as presented here, therefore, could contribute to modeling studies of the processes of ozone loss chemistry and projection of ozone recovery.

REFERENCES

(1) Farman, J. C.; Gardiner, B. G.; Shanklin, J. D. Large Losses of Total Ozone in Antarctica Reveal Seasonal ClOx/NOx Interaction. *Nature* **1985**, *315*, 207–210. DOI: 10.1038/315207a0.

(2) Molina, M. J.; Rowland, F. S. Stratospheric Sink for Chlorofluoromethanes: Chlorine Atom-Catalysed Destruction of Ozone. *Nature* **1974**, *249*, 810–812. DOI: 10.1038/249810a0.

(3) Stolarski, R. S.; Cicerone, R. J. Stratospheric Chlorine: A Possible Sink for Ozone. *Can. J. Chem.* **1974**, *52*, 1615. DOI: 10.1139/v74-233.

(4) Wofsy, S. C.; McElroy, M. B.; Yung, Y. L. The Chemistry of Atmospheric Bromine. *Geophys. Res. Lett.* **1975**, *2*, 215–218. DOI: 10.1029/GL002I006P00215.

(5) McElroy, M. B.; Salawitch, R. J.; Wofsy, S. C.; Logan, J. A. Reductions of Antarctic Ozone Due to Synergistic Interactions of Chlorine and Bromine. *Nature* **1986**, *321*, 759–762. DOI: 10.1038/321759a0.

(6) Rowland, S. F. Stratospheric Ozone Depletion by Chlorofluorocarbons. *Ambio* **1990**, *19*, 281–292.

(7) Solomon, S.; Portmann, R. W.; Thompson, D. W. J. Contrasts between Antarctic and Arctic Ozone Depletion. *Proc. Natl. Acad. Sci.* **2007**, *104*, 445–449. DOI: 10.1073/PNAS.0604895104.

(8) Solomon, S.; Haskins, J.; Ivy, D. J.; Min, F. Fundamental Differences between Arctic and Antarctic Ozone Depletion. *Proc. Natl. Acad. Sci.* **2014**, *111*, 6220–6225. DOI: 10.1073/PNAS.1319307111.

(9) Schoeberl, M. R.; Hartmann, D. L. The Dynamics of the Stratospheric Polar Vortex and Its Relation to Springtime Ozone Depletions. *Science.* **1991**, *251*, 46–52. DOI: 10.1126/SCIENCE.251.4989.46.

(10) Tegtmeier, S.; Rex, M.; Wohltmann, I.; Krüger, K. Relative Importance of Dynamical and Chemical Contributions to Arctic Wintertime Ozone. *Geophys. Res. Lett.* **2008**, *35*, L17801. DOI: 10.1029/2008GL034250.

(11) Strahan, S. E.; Douglass, A. R.; Newman, P. A. The Contributions of Chemistry and Transport to Low Arctic Ozone in March 2011 Derived from Aura MLS Observations. *J. Geophys. Res. Atmos.* **2013**, *118*, 1563–1576. DOI: 10.1002/JGRD.50181.

(12) WMO (World Meteorological Organization), *Scientific Assessment of Ozone Depletion: 2018*, Global Ozone Research and Monitoring Project – Report No. 58, 588 Pp., Geneva. 2018. (accessed 09/28/2021).

(13) Portmann, R. W.; Solomon, S.; Garcia, R. R.; Thomason, L. W.; Poole, L. R.; McCormick, M. P. Role of Aerosol Variations in Anthropogenic Ozone Depletion in the Polar Regions. *J. Geophys. Res. Atmos.* **1996**, *101*, 22991–23006. DOI: 10.1029/96JD02608.

(14) Grooß, J. U.; Brautzsch, K.; Pommrich, R.; Solomon, S.; Müller, R. Stratospheric Ozone Chemistry in the Antarctic: What Determines the Lowest Ozone Values Reached and Their Recovery? *Atmos. Chem. Phys.* **2011**, *11*, 12217–12226. DOI: 10.5194/ACP-11-12217-2011.

(15) Solomon, S.; Kinnison, D.; Bandoro, J.; Garcia, R. Simulation of Polar Ozone Depletion: An Update. *J. Geophys. Res. Atmos.* **2015**, *120*, 7958–7974. DOI: 10.1002/2015JD023365.

(16) Müller, R.; Grooß, J. U.; Mannan Zafar, A.; Robrecht, S.; Lehmann, R. The Maintenance of Elevated Active Chlorine Levels in the Antarctic Lower Stratosphere through HCl Null Cycles. *Atmos. Chem. Phys.* **2018**, *18*, 2985–2997. DOI: 10.5194/ACP-18-2985-2018.

(17) Solomon, S. Stratospheric Ozone Depletion: A Review of Concepts and History. *Rev. Geophys.* **1999**, *37*, 275–316. DOI: 10.1029/1999RG900008.

(18) Müller, R.; Grooß, J. U.; Lemmen, C.; Heinze, D.; Dameris, M.; Bodeker, G. Simple Measures of Ozone Depletion in the Polar Stratosphere. *Atmos. Chem. Phys.* **2008**, *8*, 251–264. DOI: 10.5194/ACP-8-251-2008.

(19) Chipperfield, M. P.; Jones, R. L. Relative Influences of Atmospheric Chemistry and Transport on Arctic Ozone Trends. *Nat. 1999 4006744* **1999**, *400*, 551–554. DOI: 10.1038/22999.

(20) Butler, A. H.; Gerber, E. P. Optimizing the Definition of a Sudden Stratospheric Warming. *J. Clim.* **2018**, *31*, 2337–2344. DOI: 10.1175/JCLI-D-17-0648.1.

(21) Kuttippurath, J.; Nikulin, G. Atmospheric Chemistry and Physics. *Atmos. Chem. Phys* **2012**, *12*, 8115–8129. DOI: 10.5194/acp-12-8115-2012.

(22) Manney, G. L.; Lawrence, Z. D.; Santee, M. L.; Read, W. G.; Livesey, N. J.; Lambert, A.; Froidevaux, L.; Pumphrey, H. C.; Schwartz, M. J. A Minor Sudden Stratospheric Warming with a Major Impact: Transport and Polar Processing in the 2014/2015 Arctic Winter. *Geophys. Res. Lett.* **2015**, *42*, 7808–7816. DOI: 10.1002/2015GL065864.

(23) De La Cámara, A.; Abalos, M.; Hitchcock, P.; Calvo, N.; Garcia, R. R. Response of Arctic Ozone to Sudden Stratospheric Warmings. *Atmos. Chem. Phys.* **2018**, *18*, 16499–16513. DOI: 10.5194/acp-18-16499-2018.

(24) Müller, R.; Crutzen, P. J.; Grooβ, J.-U.; Bürhl, C.; Russell, J. M.; Gernandt, H.; McKenna, D. S.; Tuck, A. F. Severe Chemical Ozone Loss in the Arctic during the Winter of 1995–96. *Nature* **1997**, *389*, 709–712. DOI: 10.1038/39564.

(25) Pawson, S.; Naujokat, B. The Cold Winters of the Middle 1990s in the Northern Lower Stratosphere. *J. Geophys. Res. Atmos.* **1999**, *104*, 14209–14222. DOI: 10.1029/1999JD900211.

(26) Rex, M.; Salawitch, R. J.; von der Gathen, P.; Harris, N. R. P.; Chipperfield, M. P.; Naujokat, B. Arctic Ozone Loss and Climate Change. *Geophys. Res. Lett.* **2004**, *31*, L04116. DOI: 10.1029/2003GL018844.

(27) Harris, N. R. P.; Lehmann, R.; Rex, M.; Von Der Gathen, P. A Closer Look at Arctic Ozone Loss and Polar Stratospheric Clouds. *Atmos. Chem. Phys.* **2010**, *10*, 8499–8510. DOI: 10.5194/ACP-10-8499-2010.

(28) Rex, M.; Salawitch, R. J.; Deckelmann, H.; von der Gathen, P.; Harris, N. R. P.; Chipperfield, M. P.; Naujokat, B.; Reimer, E.; Allaart, M.; Andersen, S. B.; Bevilacqua, R.; Braathen, G. O.; Claude, H.; Davies, J.; De Backer, H.; Dier, H.; Dorokhov, V.; Fast, H.; Gerding, M.; Godin-Beekmann, S.;

Hoppel, K.; Johnson, B.; Kyrö, E.; Litynska, Z.; Moore, D.; Nakane, H.; Parrondo, M. C.; Risley, A. D.; Skrivankova, P.; Stübi, R.; Viatte, P.; Yushkov, V.; Zerefos, C. Arctic Winter 2005: Implications for Stratospheric Ozone Loss and Climate Change. *Geophys. Res. Lett.* 2006, *33*, L23808. DOI: 10.1029/2006GL026731.

(29) Pommereau, J. P.; Goutail, F.; Lefèvre, F.; Pazmino, A.; Adams, C.; Dorokhov, V.; Eriksen, P.; Kivi, R.; Stebel, K.; Zhao, X.; Van Roozendael, M. Why Unprecedented Ozone Loss in the Arctic in 2011? Is It Related to Climate Change? *Atmos. Chem. Phys.* 2013, *13*, 5299–5308. DOI: 10.5194/ACP-13-5299-2013.

(30) Shindell, D. T.; Rind, D.; Lonergan, P. Increased Polar Stratospheric Ozone Losses and Delayed Eventual Recovery Owing to Increasing Greenhouse-Gas Concentrations. *Nature* 1998, *392*, 589–592. DOI: 10.1038/33385.

(31) Langematz, U. An Estimate of the Impact of Observed Ozone Losses on Stratospheric Temperature. *Geophys. Res. Lett.* 2000, *27*, 2077–2080. DOI: 10.1029/2000GL011440.

(32) WMO (World Meteorological Organization), *Scientific Assessment of Ozone Depletion: 2002,* Global Ozone Research and Monitoring Project - Report No. 47, 498pp; Geneva, 2003. (accessed 09/28/2021).

(33) Stolarski, R. S.; Douglass, A. R.; Newman, P. A.; Pawson, S.; Schoeberl, M. R. Relative Contribution of Greenhouse Gases and Ozone-Depleting Substances to Temperature Trends in the Stratosphere: A Chemistry–Climate Model Study. *J. Clim.* 2010, *23*, 28–42. DOI: 10.1175/2009JCLI2955.1.

(34) von der Gathen, P.; Kivi, R.; Wohltmann, I.; Salawitch, R. J.; Rex, M. Climate Change Favours Large Seasonal Loss of Arctic Ozone. *Nat. Commun.* 2021, *12*, 1–17. DOI: 10.1038/s41467-021-24089-6.

(35) Sinnhuber, B. M.; Stiller, G.; Ruhnke, R.; Von Clarmann, T.; Kellmann, S.; Aschmann, J. Arctic Winter 2010/2011 at the Brink of an Ozone Hole. *Geophys. Res. Lett.* 2011, *38*, L24814. DOI: 10.1029/2011GL049784.

(36) Bohlinger, P.; Sinnhuber, B. M.; Ruhnke, R.; Kirner, O. Radiative and Dynamical Contributions to Past and Future Arctic Stratospheric Temperature Trends. *Atmos. Chem. Phys.* 2014, *14*, 1679–1688. DOI: 10.5194/ACP-14-1679-2014.

(37) Langematz, U.; Meul, S.; Grunow, K.; Romanowsky, E.; Oberländer, S.; Abalichin, J.; Kubin, A. Future Arctic Temperature and Ozone: The Role of Stratospheric Composition Changes. *J. Geophys. Res. Atmos.* 2014, *119*, 2092–2112. DOI: 10.1002/2013JD021100.

(38) Hu, D.; Guan, Z.; Tian, W.; Ren, R. Recent Strengthening of the Stratospheric Arctic Vortex

Response to Warming in the Central North Pacific. *Nat. Commun.* 2018, *9,* 1697. DOI: 10.1038/s41467-018-04138-3.

(39) Hurwitz, M. M.; Newman, P. A.; Garfinkel, C. I. On the Influence of North Pacific Sea Surface Temperature on the Arctic Winter Climate. *J. Geophys. Res.* 2012, *117*, D19110. DOI: 10.1029/2012JD017819.

(40) Woo, S.-H.; Sung, M.-K.; Son, S.-W.; Kug, J.-S. Connection between Weak Stratospheric Vortex Events and the Pacific Decadal Oscillation. *Clim. Dyn.* 2015, *45*, 3481–3492. DOI: 10.1007/S00382-015-2551-Z.

(41) Liu, M.; Hu, D.; Zhang, F. Connections Between Stratospheric Ozone Concentrations Over the Arctic and Sea Surface Temperatures in the North Pacific. *J. Geophys. Res. Atmos.* 2020, *125*, e2019JD031690. DOI: 10.1029/2019JD031690.

(42) Popp, P. J.; Northway, M. J.; Holecek, J. C.; Gao, R. S.; Fahey, D. W.; Elkins, J. W.; Hurst, D. F.; Romashkin, P. A.; Toon, G. C.; Sen, B.; Schauffler, S. M.; Salawitch, R. J.; Webster, C. R.; Herman, R. L.; Jost, H.; Bui, T. P.; Newman, P. A.; Lait, L. R. Severe and Extensive Denitrification in the 1999–2000 Arctic Winter Stratosphere. *Geophys. Res. Lett.* 2001, *28*, 2875–2878. DOI: 10.1029/2001GL013132.

(43) Tilmes, S.; Müller, R.; Grooß, J. U.; Russell, J. M. Ozone Loss and Chlorine Activation in the Arctic Winters 1991-2003 Derived with the Tracer-Tracer Correlations. *Atmos. Chem. Phys.* 2004, *4*, 2181–2213. DOI: 10.5194/ACP-4-2181-2004.

(44) Manney, G. L.; Santee, M. L.; Rex, M.; Livesey, N. J.; Pitts, M. C.; Veefkind, P.; Nash, E. R.; Wohltmann, I.; Lehmann, R.; Froidevaux, L.; Poole, L. R.; Schoeberl, M. R.; Haffner, D. P.; Davies, J.; Dorokhov, V.; Gernandt, H.; Johnson, B.; Kivi, R.; Kyrö, E.; Larsen, N.; Levelt, P. F.; Makshtas, A.; McElroy, C. T.; Nakajima, H.; Parrondo, M. C.; Tarasick, D. W.; von der Gathen, P.; Walker, K. A.; Zinoviev, N. S. Unprecedented Arctic Ozone Loss in 2011. *Nat. 2011* 2011, *478*, 469–475. DOI: 10.1038/nature10556.

(45) Coy, L.; Nash, E. R.; Newman, P. A. Meteorology of the Polar Vortex: Spring 1997. *Geophys. Res. Lett.* 1997, *24*, 2693–2696. DOI: 10.1029/97GL52832.

(46) Manney, G. L.; Froidevaux, L.; Santee, M. L.; Zurek, R. W.; Waters, J. W. MLS Observations of Arctic Ozone Loss in 1996–97. *Geophys. Res. Lett.* 1997, *24*, 2697–2700. DOI: 10.1029/97GL52827.

(47) Santee, M. L.; Manney, G. L.; Froidevaux, L.; Zurek, R. W.; Waters, J. W. MLS Observations of ClO and HNO3 in the 1996–97 Arctic Polar Vortex. *Geophys. Res. Lett.* 1997, *24*, 2713–2716. DOI: 10.1029/97GL52830.

(48) Kuttippurath, J.; Godin-Beekmann, S.; Lefevre, F.; Nikulin, G.; Santee, M. L.; Froidevaux, L. Record-Breaking Ozone Loss in the Arctic Winter 2010/2011: Comparison with 1996/1997. *Atmos. Chem. Phys.* 2012, *12*, 7073–7085. DOI: 10.5194/ACP-12-7073-2012.

(49) Hommel, R.; Eichmann, K. U.; Aschmann, J.; Bramstedt, K.; Weber, M.; Von Savigny, C.; Richter, A.; Rozanov, A.; Wittrock, F.; Khosrawi, F.; Bauer, R.; Burrows, J. P. Chemical Ozone Loss and Ozone Mini-Hole Event during the Arctic Winter 2010/2011 as Observed by SCIAMACHY and GOME-2. *Atmos. Chem. Phys.* 2014, *14*, 3247–3276. DOI: 10.5194/ACP-14-3247-2014.

(50) Manney, G. L.; Lawrence, Z. D. The Major Stratospheric Final Warming in 2016: Dispersal of Vortex Air and Termination of Arctic Chemical Ozone Loss. *Atmos. Chem. Phys.* 2016, *16*, 15371–15396. DOI: 10.5194/ACP-16-15371-2016.

(51) Matthias, V.; Dörnbrack, A.; Stober, G. The Extraordinarily Strong and Cold Polar Vortex in the Early Northern Winter 2015/2016. *Geophys. Res. Lett.* 2016, *43*, 12287–12294. DOI: 10.1002/2016GL071676.

(52) Khosrawi, F.; Kirner, O.; Sinnhuber, B. M.; Johansson, S.; Höpfner, M.; Santee, M. L.; Froidevaux, L.; Ungermann, J.; Ruhnke, R.; Woiwode, W.; Oelhaf, H.; Braesicke, P. Denitrification, Dehydration and Ozone Loss during the 2015/2016 Arctic Winter. *Atmos. Chem. Phys.* 2017, *17*, 12893–12910. DOI: 10.5194/ACP-17-12893-2017.

(53) Lawrence, Z. D.; Perlwitz, J.; Butler, A. H.; Manney, G. L.; Newman, P. A.; Lee, S. H.; Nash, E. R. The Remarkably Strong Arctic Stratospheric Polar Vortex of Winter 2020: Links to Record-Breaking Arctic Oscillation and Ozone Loss. *J. Geophys. Res. Atmos.* 2020, *125*, e2020JD033271. DOI: 10.1029/2020JD033271.

(54) Inness, A.; Chabrillat, S.; Flemming, J.; Huijnen, V.; Langenrock, B.; Nicolas, J.; Polichtchouk, I.; Razinger, M. Exceptionally Low Arctic Stratospheric Ozone in Spring 2020 as Seen in the CAMS Reanalysis. *J. Geophys. Res. Atmos.* 2020, *125*, e2020JD033563. DOI: 10.1029/2020JD033563.

(55) Manney, G. L.; Livesey, N. J.; Santee, M. L.; Froidevaux, L.; Lambert, A.; Lawrence, Z. D.; Millán, L. F.; Neu, J. L.; Read, W. G.; Schwartz, M. J.; Fuller, R. A. Record-Low Arctic Stratospheric Ozone in 2020: MLS Observations of Chemical Processes and Comparisons With Previous Extreme Winters. *Geophys. Res. Lett.* 2020, *47*, e2020GL089063. DOI: 10.1029/2020GL089063.

(56) Wohltmann, I.; von der Gathen, P.; Lehmann, R.; Maturilli, M.; Deckelmann, H.; Manney, G. L.; Davies, J.; Tarasick, D.; Jepsen, N.; Kivi, R.; Lyall, N.; Rex, M. Near-Complete Local Reduction of Arctic Stratospheric Ozone by Severe Chemical Loss in Spring 2020. *Geophys. Res. Lett.* 2020, *47*, e2020GL089547. DOI: 10.1029/2020GL089547.

(57) Kuttippurath, J.; Feng, W.; Müller, R.; Kumar, P.; Raj, S.; Gopikrishnan, G. P.; Roy, R. Exceptional Loss in Ozone in the Arctic Winter/Spring of 2019/2020. *Atmos. Chem. Phys.* **2021**, *21*, 14019–14037. DOI: 10.5194/ACP-21-14019-2021.

(58) Weber, M.; Arosio, C.; Feng, W.; Dhomse, S. S.; Chipperfield, M. P.; Meier, A.; Burrows, J. P.; Eichmann, K. U.; Richter, A.; Rozanov, A. The Unusual Stratospheric Arctic Winter 2019/20: Chemical Ozone Loss From Satellite Observations and TOMCAT Chemical Transport Model. *J. Geophys. Res. Atmos.* **2021**, *126*, e2020JD034386. DOI: 10.1029/2020JD034386.

(59) Rao, J.; Garfinkel, C. I.; White, I. P. Predicting the Downward and Surface Influence of the February 2018 and January 2019 Sudden Stratospheric Warming Events in Subseasonal to Seasonal (S2S) Models. *J. Geophys. Res. Atmos.* **2020**, *125*, e2019JD031919. DOI: 10.1029/2019JD031919.

(60) Feng, W.; Dhomse, S. S.; Arosio, C.; Weber, M.; Burrows, J. P.; Santee, M. L.; Chipperfield, M. P. Arctic Ozone Depletion in 2019/20: Roles of Chemistry, Dynamics and the Montreal Protocol. *Geophys. Res. Lett.* **2021**, *48*, e2020GL091911. DOI: 10.1029/2020GL091911.

(61) Grooß, J.-U.; Müller, R. Simulation of Record Arctic Stratospheric Ozone Depletion in 2020. *J. Geophys. Res. Atmos.* **2021**, *126*, e2020JD033339. DOI: 10.1029/2020JD033339.

(62) Kuttippurath, J.; Kumar, P.; Nair, P. J.; Pandey, P. C. Emergence of Ozone Recovery Evidenced by Reduction in the Occurrence of Antarctic Ozone Loss Saturation. *npj Clim. Atmos. Sci.* **2018**, *1,* 42. DOI: 10.1038/s41612-018-0052-6.

(63) Livesey, N. J. .; Read, W. G.; Wagner, P. A.; Froidevaux, L.; Lambert, A.; Manney, G. L.; Valle, L. F. M.; Pumphrey, H. C.; Santee, M. L.; Schwartz, M. J.; Wang, S.; Fuller, R. A.; Jarnot, R. F.; Knosp, B. W.; Martinez, E.; Lay, R. R. *Version 4.2x Level 2 and 3 data quality and description document, JPL D-33509 Rev. E*. Jet Propulsion Laboratory, California Institute of Technology, Pasadena, California, 2020. https://mls.jpl.nasa.gov/data/v4-2_data_quality_document.pdf (accessed 09/28/2021).

(64) Hersbach, H.; Bell, B.; Berrisford, P.; Hirahara, S.; Horányi, A.; Muñoz-Sabater, J.; Nicolas, J.; Peubey, C.; Radu, R.; Schepers, D.; Simmons, A.; Soci, C.; Abdalla, S.; Abellan, X.; Balsamo, G.; Bechtold, P.; Biavati, G.; Bidlot, J.; Bonavita, M.; Chiara, G. De; Dahlgren, P.; Dee, D.; Diamantakis, M.; Dragani, R.; Flemming, J.; Forbes, R.; Fuentes, M.; Geer, A.; Haimberger, L.; Healy, S.; Hogan, R. J.; Hólm, E.; Janisková, M.; Keeley, S.; Laloyaux, P.; Lopez, P.; Lupu, C.; Radnoti, G.; Rosnay, P. de; Rozum, I.; Vamborg, F.; Villaume, S.; Thépaut, J.-N. The ERA5 Global Reanalysis. *Q. J. R. Meteorol. Soc.* **2020**, *146*, 1999–2049. DOI: 10.1002/QJ.3803.

(65) Nash, E. R.; Newman, P. A.; Rosenfield, J. E.; Schoeberl, M. R. An Objective Determination of the Polar Vortex Using Ertel's Potential Vorticity. *J. Geophys. Res. Atmos.* **1996**, *101*, 9471–9478. DOI:

10.1029/96JD00066.

(66) Bremer, H.; König, M. von; Kleinböhl, A.; Küllmann, H.; Künzi, K.; Bramstedt, K.; Burrows, J. P.; Eichmann, K.-U.; Weber, M.; Goede, A. P. H. Ozone Depletion Observed by the Airborne Submillimeter Radiometer (ASUR) during the Arctic Winter 1999/2000. *J. Geophys. Res. Atmos.* 2002, *107*, SOL 19-1-SOL 19-7. DOI: 10.1029/2001JD000546.

(67) Rex, M.; Salawitch, R. J.; Harris, N. R. P.; Gathen, P. von der; Braathen, G. O.; Schulz, A.; Deckelmann, H.; Chipperfield, M.; Sinnhuber, B.-M.; Reimer, E.; Alfier, R.; Bevilacqua, R.; Hoppel, K.; Fromm, M.; Lumpe, J.; Küllmann, H.; Kleinböhl, A.; Bremer, H.; König, M. von; Künzi, K.; Toohey, D.; Vömel, H.; Richard, E.; Aikin, K.; Jost, H.; Greenblatt, J. B.; Loewenstein, M.; Podolske, J. R.; Webster, C. R.; Flesch, G. J.; Scott, D. C.; Herman, R. L.; Elkins, J. W.; Ray, E. A.; Moore, F. L.; Hurst, D. F.; Romashkin, P.; Toon, G. C.; Sen, B.; Margitan, J. J.; Wennberg, P.; Neuber, R.; Allart, M.; Bojkov, B. R.; Claude, H.; Davies, J.; Davies, W.; Backer, H. De; Dier, H.; Dorokhov, V.; Fast, H.; Kondo, Y.; Kyrö, E.; Litynska, Z.; Mikkelsen, I. S.; Molyneux, M. J.; Moran, E.; Nagai, T.; Nakane, H.; Parrondo, C.; Ravegnani, F.; Skrivankova, P.; Viatte, P.; Yushkov, V. Chemical Depletion of Arctic Ozone in Winter 1999/2000. *J. Geophys. Res. Atmos.* 2002, *107*, SOL 18-1. DOI: 10.1029/2001JD000533.

(68) Jin, J. J.; Semeniuk, K.; Manney, G. L.; Jonsson, A. I.; Beagley, S. R.; McConnell, J. C.; Dufour, G.; Nassar, R.; Boone, C. D.; Walker, K. A.; Bernath, P. F.; Rinsland, C. P. Severe Arctic Ozone Loss in the Winter 2004/2005: Observations from ACE-FTS. *Geophys. Res. Lett.* 2006, *33*, L15801. DOI: 10.1029/2006GL026752.

(69) Griffin, D.; Walker, K. A.; Wohltmann, I.; Dhomse, S. S.; Rex, M.; Chipperfield, M. P.; Feng, W.; Manney, G. L.; Liu, J.; Tarasick, D. Stratospheric Ozone Loss in the Arctic Winters between 2005 and 2013 Derived with ACE-FTS Measurements. *Atmos. Chem. Phys.* 2019, *19*, 577–601. DOI: 10.5194/ACP-19-577-2019.

(70) Feng, W.; Chipperfield, M. P.; Davies, S.; von der Gathen, P.; Kyrö, E.; Volk, C. M.; Ulanovsky, A.; Belyaev, G. Large Chemical Ozone Loss in 2004/2005 Arctic Winter/Spring. *Geophys. Res. Lett.* 2007, *34*, L09803. DOI: 10.1029/2006GL029098.

(71) Zhang, J.; Tian, W.; Xie, F.; Chipperfield, M. P.; Feng, W.; Son, S.-W.; Abraham, N. L.; Archibald, A. T.; Bekki, S.; Butchart, N.; Deushi, M.; Dhomse, S.; Han, Y.; Jöckel, P.; Kinnison, D.; Kirner, O.; Michou, M.; Morgenstern, O.; O'Connor, F. M.; Pitari, G.; Plummer, D. A.; Revell, L. E.; Rozanov, E.; Visioni, D.; Wang, W.; Zeng, G. Stratospheric Ozone Loss over the Eurasian Continent Induced by the Polar Vortex Shift. *Nat. Commun.* 2018, *9*, 206. DOI: 10.1038/s41467-017-02565-2.

(72) Gelaro, R.; McCarty, W.; Suárez, M. J.; Todling, R.; Molod, A.; Takacs, L.; Randles, C. A.; Darmenov, A.; Bosilovich, M. G.; Reichle, R.; Wargan, K.; Coy, L.; Cullather, R.; Draper, C.; Akella, S.; Buchard, V.; Conaty, A.; Silva, A. M. da; Gu, W.; Kim, G.-K.; Koster, R.; Lucchesi, R.; Merkova, D.; Nielsen, J. E.; Partyka, G.; Pawson, S.; Putman, W.; Rienecker, M.; Schubert, S. D.; Sienkiewicz, M.; Zhao, B. The Modern-Era Retrospective Analysis for Research and Applications, Version 2 (MERRA-2). *J. Clim.* 2017, *30*, 5419–5454. DOI: 10.1175/JCLI-D-16-0758.1.

(73) McCormick, M. P.; Steele, H. M.; Hamill, P.; Chu, W. P.; Swissler, T. J. Polar Stratospheric Cloud Sightings by SAM II . *J. Atmos. Sci.* 1982, *39*, 1387–1397. DOI: 10.1175/1520-0469(1982)039%3C1387:PSCSBS%3E2.0.CO;2

(74) Varotsos, C. A.; Cracknell, A. P.; Tzanis, C. The Exceptional Ozone Depletion over the Arctic in January–March 2011. *Remote Sens. Lett.* 2011, *3*, 343–352. DOI: 10.1080/01431161.2011.597792.

(75) Dameris, M.; G. Loyola, D.; Nützel, M.; Coldewey-Egbers, M.; Lerot, C.; Romahn, F.; Van Roozendael, M. Record Low Ozone Values over the Arctic in Boreal Spring 2020. *Atmos. Chem. Phys.* 2021, *21*, 617–633. DOI: 10.5194/ACP-21-617-2021.

(76) Alwarda, R.; Bognar, K.; Strong, K.; Chipperfield, M.; Dhomse, S.; Drummond, J.; Feng, W.; Fioletov, V.; Goutail, F.; Herrera, B.; Manney, G.; McCullough, E.; Millan, L.; Pazmino, A.; Walker, K.; Wizenberg, T.; Zhao, X. Record Springtime Stratospheric Ozone Depletion at 80°N in 2020. In *EGU General Assembly 2021, online, 19–30 Apr 2021*; 2021. DOI: 10.5194/egusphere-egu21-8892.

(77) DeLand, M. T.; Bhartia, P. K.; Kramarova, N.; Chen, Z. OMPS LP Observations of PSC Variability During the NH 2019–2020 Season. *Geophys. Res. Lett.* 2020, *47*, e2020GL090216. DOI: 10.1029/2020GL090216.

(78) Curbelo, J.; Chen, G.; Mechoso, C. R. Lagrangian Analysis of the Northern Stratospheric Polar Vortex Split in April 2020. *Geophys. Res. Lett.* 2021, *48*, e2021GL093874. DOI: 10.1029/2021GL093874.

(79) Rao, J.; Garfinkel, C. I. Arctic Ozone Loss in March 2020 and Its Seasonal Prediction in CFSv2: A Comparative Study With the 1997 and 2011 Cases. *J. Geophys. Res. Atmos.* 2020, *125*, e2020JD033524. DOI: 10.1029/2020JD033524.

(80) Lee, S. H.; Lawrence, Z. D.; Butler, A. H.; Karpechko, A. Y. Seasonal Forecasts of the Exceptional Northern Hemisphere Winter of 2020. *Geophys. Res. Lett.* 2020, *47*, e2020GL090328. DOI: 10.1029/2020GL090328.

(81) Garfinkel, C. I.; Shaw, T. A.; Hartmann, D. L.; Waugh, D. W. Does the Holton–Tan Mechanism Explain How the Quasi-Biennial Oscillation Modulates the Arctic Polar Vortex? *J. Atmos. Sci.* 2012,

69, 1713–1733. DOI: 10.1175/JAS-D-11-0209.1.

(82) Cohen, J.; Furtado, J. C.; Jones, J.; Barlow, M.; Whittleston, D.; Entekhabi, D. Linking Siberian Snow Cover to Precursors of Stratospheric Variability. *J. Clim.* **2014**, *27*, 5422–5432. DOI: 10.1175/JCLI-D-13-00779.1.

(83) Domeisen, D. I. V.; Garfinkel, C. I.; Butler, A. H. The Teleconnection of El Niño Southern Oscillation to the Stratosphere. *Rev. Geophys.* **2019**, *57*, 5–47. DOI: 10.1029/2018RG000596.

(84) Holton, J. R.; Tan, H.-C. The Influence of the Equatorial Quasi-Biennial Oscillation on the Global Circulation at 50 Mb. *J. Atmos. Sci.* **1980**, *37*, 2200–2208. DOI: 10.1175/1520-0469(1980)037<2200:tioteq>2.0.co;2.

(85) Hurwitz, M. M.; Newman, P. A.; Garfinkel, C. I. The Arctic Vortex in March 2011: A Dynamical Perspective. *Atmos. Chem. Phys.* **2011**, *11*, 11447–11453. DOI: 10.5194/ACP-11-11447-2011.

(86) Rao, J.; Ren, R.; Xia, X.; Shi, C.; Guo, D. Combined Impact of El Niño–Southern Oscillation and Pacific Decadal Oscillation on the Northern Winter Stratosphere. *Atmosphere.* **2019**, *10*, 211. DOI: 10.3390/ATMOS10040211.

(87) Adams, C.; Strong, K.; Zhao, X.; Bassford, M. R.; Chipperfield, M. P.; Daffer, W.; Drummond, J. R.; Farahani, E. E.; Feng, W.; Fraser, A.; Goutail, F.; Manney, G.; McLinden, C. A.; Pazmino, A.; Rex, M.; Walker, K. A. Severe 2011 Ozone Depletion Assessed with 11 Years of Ozone, NO 2, and OClO Measurements at 80N. *Geophys. Res. Lett.* **2012**, *39*, L05806. DOI: 10.1029/2011GL050478.

(88) Davies, S.; Chipperfield, M. P.; Carslaw, K. S.; Sinnhuber, B.-M.; Anderson, J. G.; Stimpfle, R. M.; Wilmouth, D. M.; Fahey, D. W.; Popp, P. J.; Richard, E. C.; Gathen, P. von der; Jost, H.; Webster, C. R. Modeling the Effect of Denitrification on Arctic Ozone Depletion during Winter 1999/2000. *J. Geophys. Res. Atmos.* **2002**, *107*, SOL 65-1-SOL 65-18. DOI: 10.1029/2001JD000445.

(89) Arnone, E.; Castelli, E.; Papandrea, E.; Carlotti, M.; Dinelli, B. M. Extreme Ozone Depletion in the 2010-2011 Arctic Winter Stratosphere as Observed by MIPAS/ENVISAT Using a 2-D Tomographic Approach. *Atmos. Chem. Phys.* **2012**, *12*, 9149–9165. DOI: 10.5194/ACP-12-9149-2012.

(90) Harris, N. R. P.; Rex, M.; Goutail, F.; Knudsen, B. M.; Manney, G. L.; Müller, R.; Gathen, P. von der. Comparison of Empirically Derived Ozone Losses in the Arctic Vortex. *J. Geophys. Res. Atmos.* **2002**, *107*, SOL 7-1-SOL 7-11. DOI: 10.1029/2001JD000482.

(91) Kuttippurath, J.; Goutail, F.; Pommereau, J. P.; Lefévre, F.; Roscoe, H. K.; Pazmĩno, A.; Feng, W.; Chipperfield, M. P.; Godin-Beekmann, S. Estimation of Antarctic Ozone Loss from Ground-Based Total Column Measurements. *Atmos. Chem. Phys.* **2010**, *10*, 6569–6581. DOI: 10.5194/ACP-10-6569-2010.

(92) Chipperfield, M. P. Multiannual Simulations with a Three-Dimensional Chemical Transport Model. *J. Geophys. Res. Atmos.* **1999**, *104*, 1781–1805. DOI: 10.1029/98JD02597.

(93) Livesey, N. J.; Santee, M. L.; Manney, G. L. A Match-Based Approach to the Estimation of Polar Stratospheric Ozone Loss Using Aura Microwave Limb Sounder Observations. *Atmos. Chem. Phys.* **2015**, *15*, 9945–9963. DOI: 10.5194/ACP-15-9945-2015.

(94) Neale, R. E.; Barnes, P. W.; Robson, T. M.; Neale, P. J.; Williamson, C. E.; Zepp, R. G.; Wilson, S. R.; Madronich, S.; Andrady, A. L.; Heikkilä, A. M.; Bernhard, G. H.; Bais, A. F.; Aucamp, P. J.; Banaszak, A. T.; Bornman, J. F.; Bruckman, L. S.; Byrne, S. N.; Foereid, B.; Häder, D.-P.; Hollestein, L. M.; Hou, W.-C.; Hylander, S.; Jansen, M. A. K.; Klekociuk, A. R.; Liley, J. B.; Longstreth, J.; Lucas, R. M.; Martinez-Abaigar, J.; McNeill, K.; Olsen, C. M.; Pandey, K. K.; Rhodes, L. E.; Robinson, S. A.; Rose, K. C.; Schikowski, T.; Solomon, K. R.; Sulzberger, B.; Ukpebor, J. E.; Wang, Q.-W.; Wängberg, S.-Å.; White, C. C.; Yazar, S.; Young, A. R.; Young, P. J.; Zhu, L.; Zhu, M. Environmental Effects of Stratospheric Ozone Depletion, UV Radiation, and Interactions with Climate Change: UNEP Environmental Effects Assessment Panel, Update 2020. *Photochem. Photobiol. Sci.* **2021**, *20*, 1–67. DOI: 10.1007/S43630-020-00001-X.

(95) Bernhard, G. H.; Fioletov, V. E.; Grooß, J. U.; Ialongo, I.; Johnsen, B.; Lakkala, K.; Manney, G. L.; Müller, R.; Svendby, T. Record-Breaking Increases in Arctic Solar Ultraviolet Radiation Caused by Exceptionally Large Ozone Depletion in 2020. *Geophys. Res. Lett.* **2020**, *47*, e2020GL090844. DOI: 10.1029/2020GL090844.

(96) Pommereau, J. P.; Goutail, F.; Pazmino, A.; Lefèvre, F.; Chipperfield, M. P.; Feng, W.; Van Roozendael, M.; Jepsen, N.; Hansen, G.; Kivi, R.; Bognar, K.; Strong, K.; Walker, K.; Kuzmichev, A.; Khattatov, S.; Sitnikova, V. Recent Arctic Ozone Depletion: Is There an Impact of Climate Change? Comptes Rendus - Geosci. 2018, 350 (7), 347–353. DOI: 10.1016/j.crte.2018.07.009.10.1016/j.crte.2018.07.009.

(97) Wilka, C.; Solomon, S.; Kinnison, D.; Tarasick, D. An Arctic Ozone Hole in 2020 If Not For the Montreal Protocol. *Atmos. Chem. Phys.* **2021**. DOI: 10.5194/acp-21-15771-2021.

662 **Table 1:** Comparison of different parameters related to Arctic meteorology and chemistry during the

663 winters 2011 and 2020.

Parameter	2011 Monthly Mean		2020 Monthly Mean	
	March	April	March	April
Minimum temperature (50 hPa)	191.29	198.74	190.54	202.5
60°–90°S Temperature (10 hPa)	213.22	217.14	215.31	215.48
PSC Area (460 K) (Million km^2)	5.0168	4.0466	7.1881	5.7600
PSC Volume (460 K) (Million km^3)	51.971	54.711	68.199	41.832
Total eddy heat flux (kms^{-1})	13.842	14.595	13.098	12.866
Vortex area (460 K) (Million km^2)	17.326	16.116	20.064	19.400
Vortex Edge Potential Vorticity (MPV) 1 PVU = 10^{-6} Kkg^{-1} m^2 s^{-1}	21.926	22.004	22.390	22.392
60°S zonal wind (10 hPa) (ms^{-1})	38.397	16.160	40.402	19.594
Momentum Flux at 60° (m^2s^2)	-5.6727	- 4.6488	-4.4016	-3.1005
Wave 1 Amplitude of Geopotential Height at 60° (gpm)	198.19	186.40	196.53	202.75
Wave 2 Amplitude of Geopotential Height at 60° (gpm)	198.19	185.56	196.53	206.56
Ozone Minimum (DU)	248.65	250.06	238.31	238.22

664

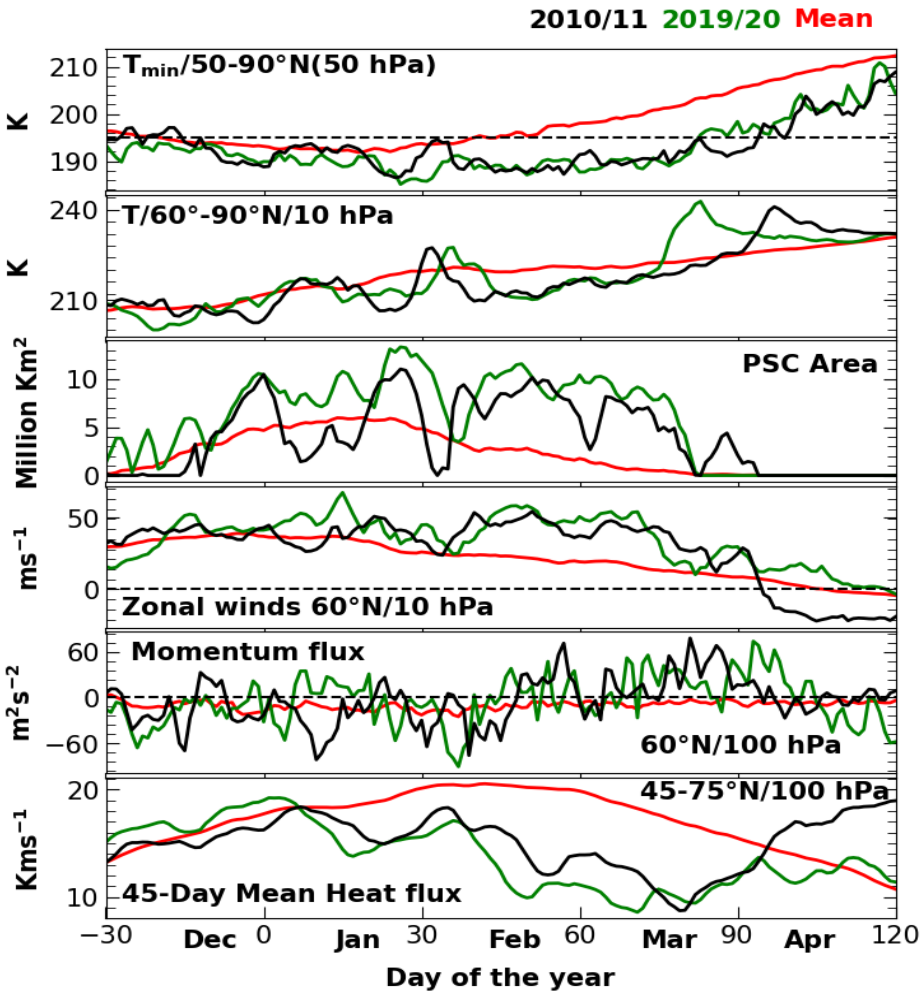

Figure 1: Meteorology of the winters. Seasonal evolution of the meteorological parameters during the winters 2011 (black) and 2020 (green). The averaged meteorological parameters for the winters from 1979 to 2020 are also shown (red).

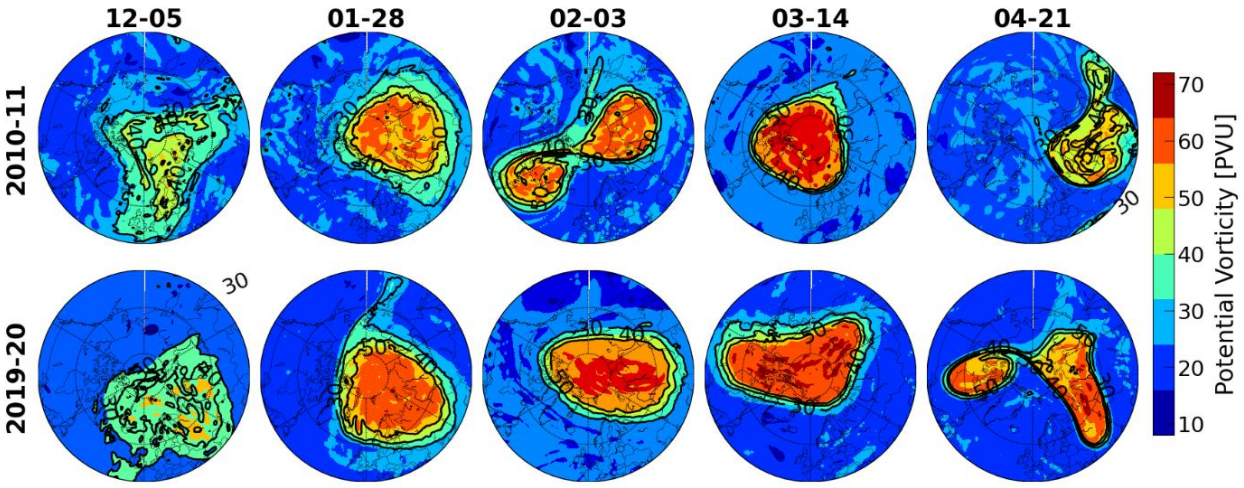

Figure 2: Temporal evolution of polar vortex. The position and strength of polar vortex in the Arctic winters 2011 and 2020 as analyzed from the ERA5 data. The vortex situation in the lower stratosphere at 460 K (~16 km), the altitude of peak ozone loss, is illustrated.

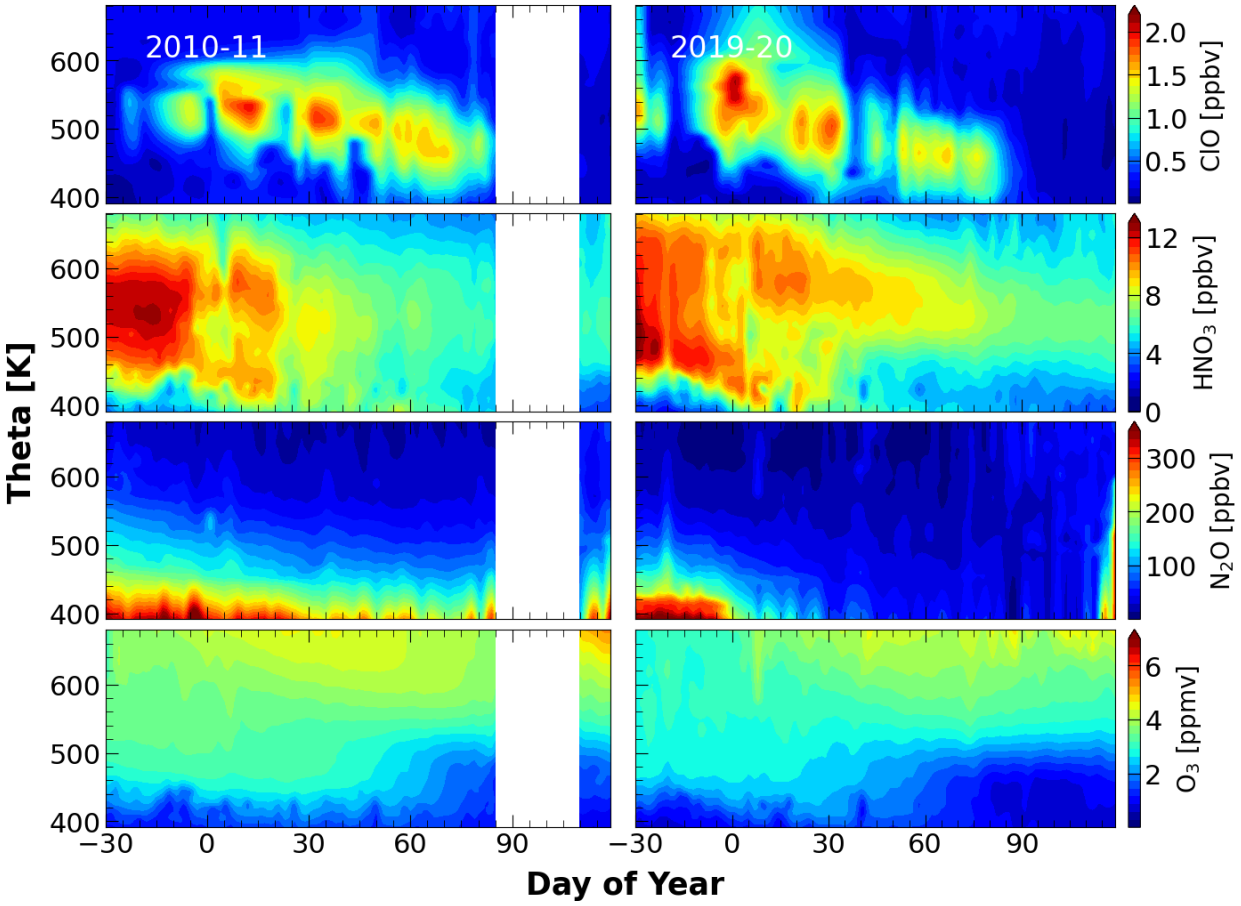

Figure 3: Chemistry of the winters. The distribution of ClO, HNO_3, N_2O, and ozone inside the polar vortex for the Arctic during winter 2020 (right) and 2011 (left). The data shown are from the Microwave Limb Sounder.

693

694

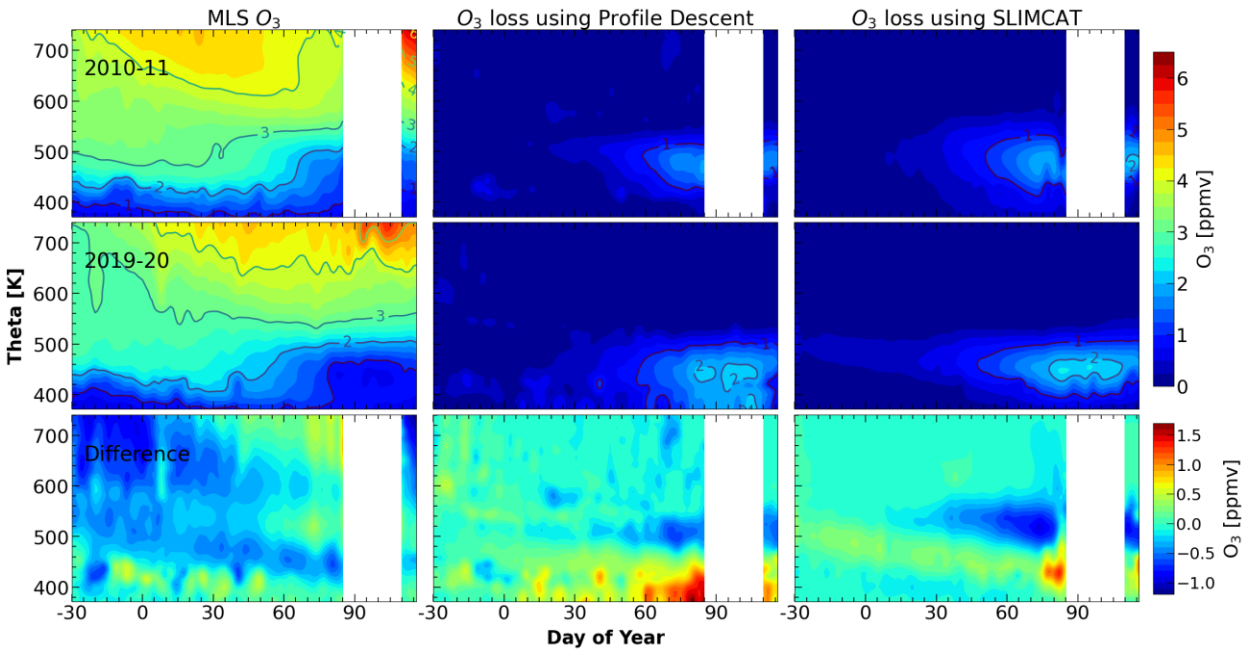

695 **Figure 4: Ozone depletion in the Arctic winter 2011 and 2020.** The ozone (left) ozone loss estimated using
696 the Microwave Limb Sounder measurements by applying the vortex descent (middle) method and passive
697 method (right) using the tracer simulations from SLIMCAT for the Arctic winters 2011 and 2020.

698

699

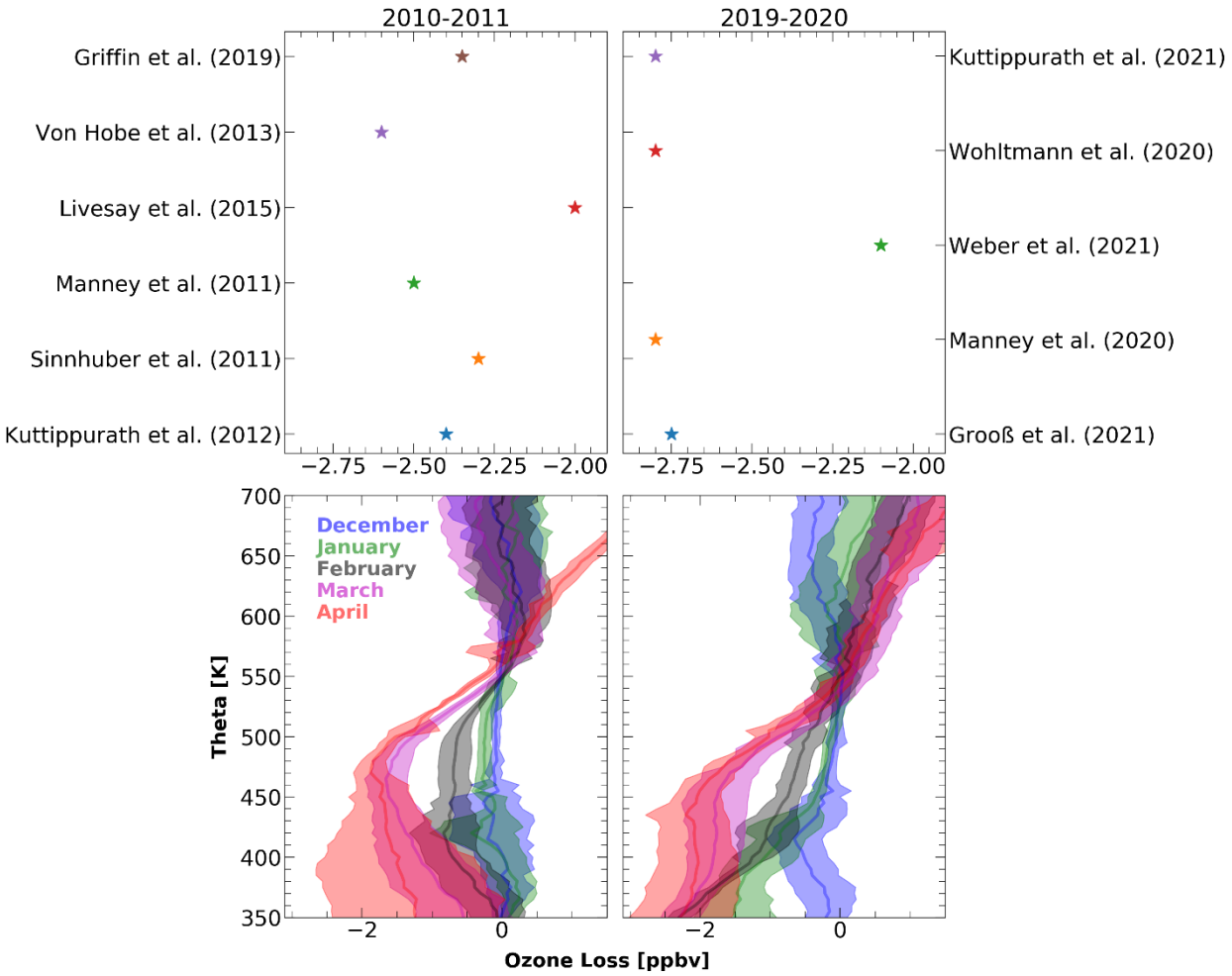

Figure 5: Ozone loss in winter months. The ozone loss estimated using the vortex descent method for each winter and spring months in 2011 (left) and 2020 (left). The ozone loss estimated in different studies for the winters 2011 and 2020 (upper panels).

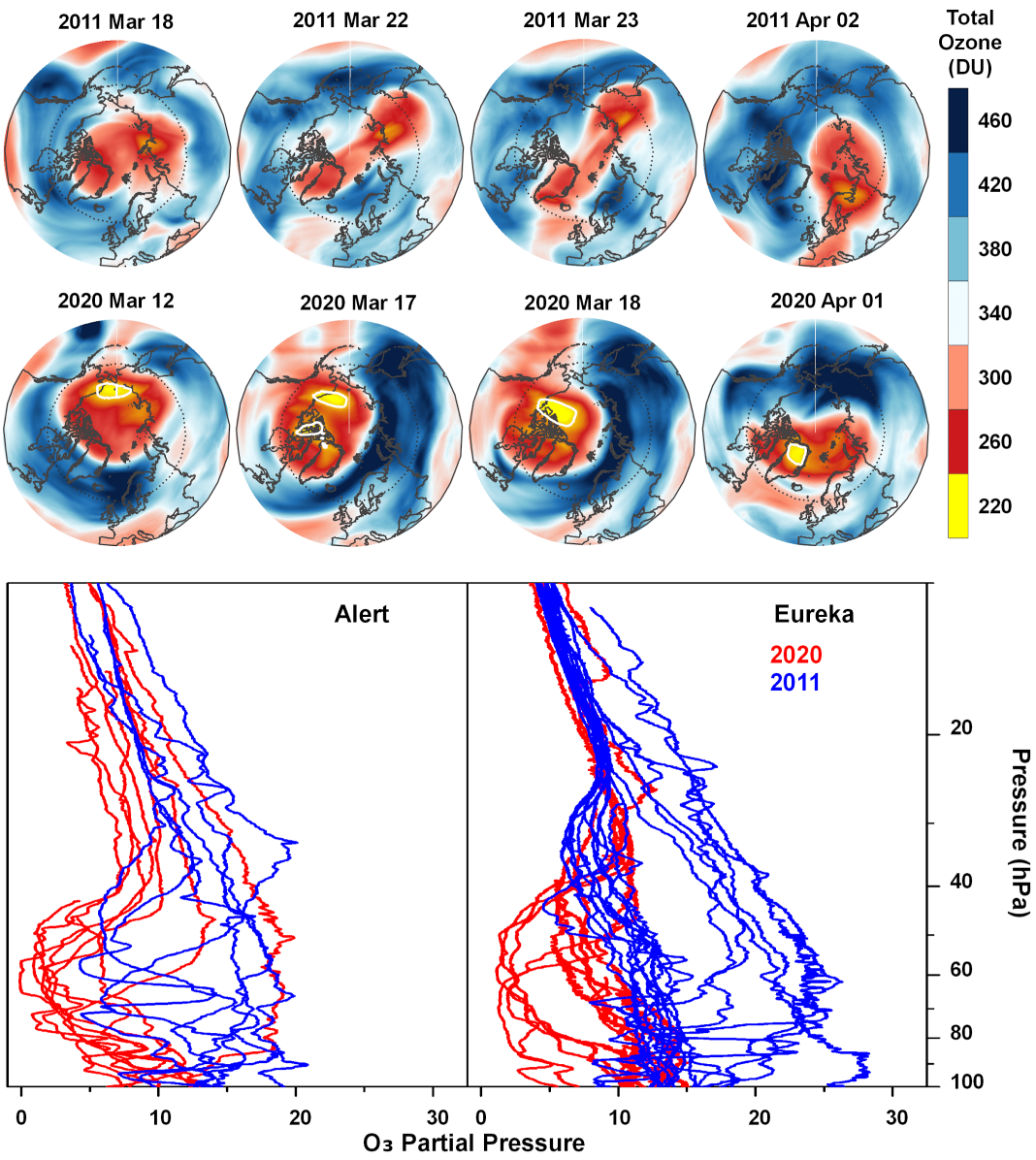

Figure 6: Total column ozone and ozone loss saturation. Total column ozone maps produced using MERRA-2 data for the Arctic winters 2011 and 2020. The total ozone values below the ozone hole criterion (220 DU) are shown in yellow contours. The ozonesonde measurements were performed at two stations in the Arctic (Eureka and Alert) during both winters (lower panels).

For TOC Only

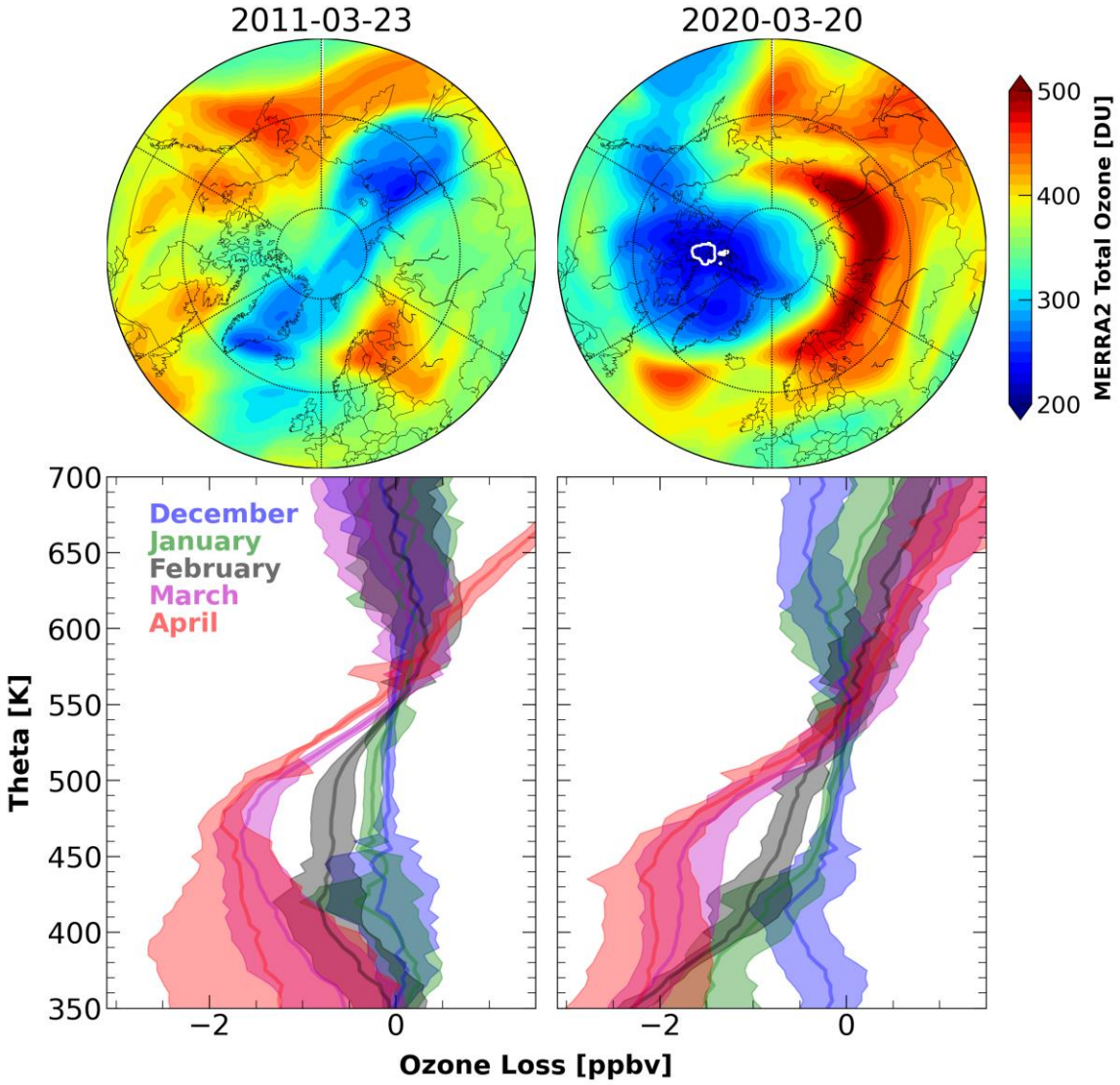

JK/2REV/V02/08022022/11pm